Molecular Cell

Short article

IκBζ is a dual-use coactivator of NF-κB and POU transcription factors

Graphical abstract

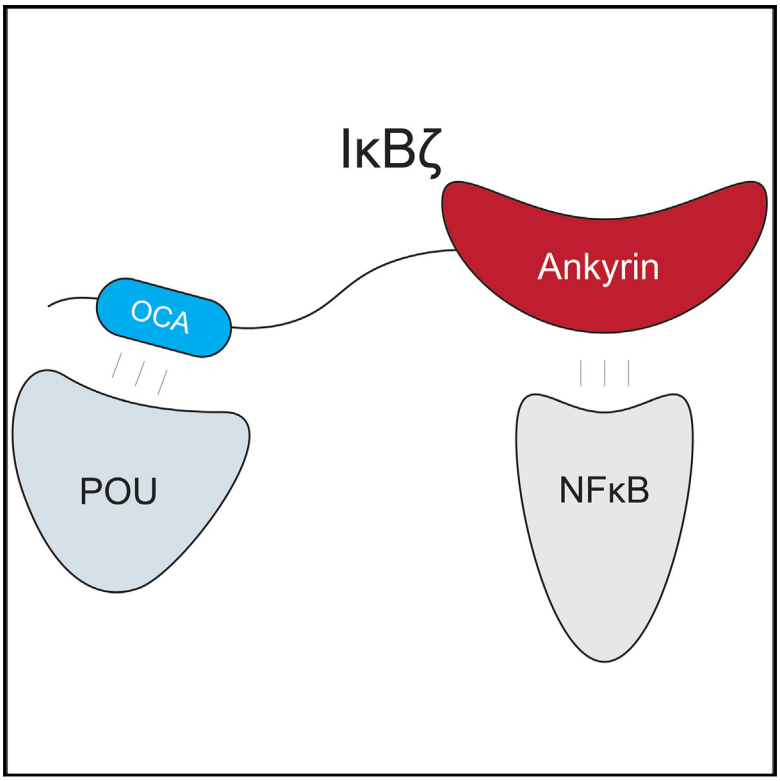

Authors

Aktan Alpsoy, Xiaoli S. Wu, Sujay Pal, ..., Osama El Demerdash, Benan Nalbant, Christopher R. Vakoc

Correspondence

vakoc@cshl.edu

In brief

Alpsoy and Wu et al. demonstrate that a well-studied NF-κB regulator, IκBζ, is also a direct binding partner and cofactor of POU transcription factors. These findings implicate IκBζ as an integrator and amplifier of two distinct families of transcription factors at inducible immune genes.

Highlights

- IκBζ interacts with POU transcription factors via a conserved OCA peptide
- IκBζ functions as a coactivator of both POU and NF-κB transcription factors
- Several immune genes require the OCA peptide of IκBζ for inducible gene activation
- Promoter sequence determines whether cooperativity exists among IκBζ, POU, and NF-κB

Alpsoy et al., 2024, Molecular Cell *84*, 1149–1157
March 21, 2024 © 2024 Elsevier Inc.
https://doi.org/10.1016/j.molcel.2024.01.007

CellPress

Molecular Cell

CellPress

Short article

IκBζ is a dual-use coactivator of NF-κB and POU transcription factors

Aktan Alpsoy,[1,2] Xiaoli S. Wu,[1,2] Sujay Pal,[1] Olaf Klingbeil,[1] Pramod Kumar,[1] Osama El Demerdash,[1] Benan Nalbant,[1] and Christopher R. Vakoc[1,3,*]

[1]Cold Spring Harbor Laboratory, Cold Spring Harbor, NY 11724, USA

[2]These authors contributed equally

[3]Lead contact

*Correspondence: vakoc@cshl.edu

https://doi.org/10.1016/j.molcel.2024.01.007

SUMMARY

OCA-B, OCA-T1, and OCA-T2 belong to a family of coactivators that bind to POU transcription factors (TFs) to regulate gene expression in immune cells. Here, we identify IκBζ (encoded by the *NFKBIZ* gene) as an additional coactivator of POU TFs. Although originally discovered as an inducible regulator of NF-κB, we show here that IκBζ shares a microhomology with OCA proteins and uses this segment to bind to POU TFs and octamer-motif-containing DNA. Our functional experiments suggest that IκBζ requires its interaction with POU TFs to coactivate immune-related genes. This finding is reinforced by epigenomic analysis of *MYD88*^{L265P}-mutant lymphoma cells, which revealed colocalization of IκBζ with the POU TF OCT2 and NF-κB:p50 at hundreds of DNA elements harboring octamer and κB motifs. These results suggest that IκBζ is a transcriptional coactivator that can amplify and integrate the output of NF-κB and POU TFs at inducible genes in immune cells.

INTRODUCTION

A fundamental feature of immune cells is their ability to rapidly implement transcriptional changes in response to encounters with extracellular cytokines or pathogens. Critical to such transcriptional responses are signal-inducible transcription factors (TFs), which include nuclear factor κB (NF-κB) as a prominent example.[1] Comprising heterodimers or homodimers of p65, RelB, c-Rel, p50, and p52 proteins, NF-κB is prevented from binding to κB DNA sequences by its interaction with inhibitor of nuclear factor kappa B (IκB) proteins, which can sequester NF-κB dimers in the cytoplasm.[1,2] In the classical NF-κB pathway, engagement of receptors of inflammatory signals leads to inhibitor of nuclear factor kappa B kinase (IKK)-dependent phosphorylation of IκB proteins, which triggers their degradation by the ubiquitin-proteasome system.[3] This mechanism allows for inducible entry of NF-κB into the nucleus, where it binds to κB motifs present at promoter and enhancer DNA elements to activate hundreds of downstream target genes. Importantly, during an immune response, the output of NF-κB is integrated with other inducible TFs, including signal transducer and activator of transcription (STAT),[4] activator protein 1 (AP-1),[5] and pit-oct-unc (POU) proteins.[6–8]

Among the eight IκB proteins (defined by having NF-κB-binding ankyrin repeat domains), inhibitor of nuclear factor kappa B zeta (IκBζ) has long been noted to exhibit atypical functionalities.[9] Although IκBα/β/ε become degraded by inflammatory cytokine signaling, many of these same signals (e.g., lipopolysaccharide (LPS), interleukin [IL]-1β, and IL-17) elevate IκBζ expression by transcriptional and post-transcriptional mechanisms.[10–14] In addition, IκBζ differs from IκBα/β/ε by localizing to the nucleus[12] and by binding to p50/p50 NF-κB homodimers on DNA.[15,16] Through the interaction with p50, IκBζ can function as a transcriptional coactivator of NF-κB target genes, such as *IL-6*.[16,17] Consistent with this model, IκBζ (gene symbol: *Nfkbiz*)-deficient mice exhibit impaired cytokine production in immune cells, which mirrors defects seen in p50-deficient cells.[17] Evidence also exists that IκBζ inhibits the p65 subunit of NF-κB,[12,13,18] which may lead to enhanced inflammation in IκBζ-deficient epithelial tissues.[19] However, some attributes of IκBζ function have been difficult to explain by NF-κB regulation alone, such as the selective deficit in Th17 T cell differentiation observed in IκBζ-deficient mice.[20] This has led to speculation that IκBζ can function as a cofactor of additional TFs with immune-related functions.

POU TFs OCT1/*POU2F1* and OCT2/*POU2F2* perform important roles in development, as well in the activation of inducible genes in immune cells. Despite its ubiquitous expression across cell types, several studies have shown OCT1 to be a powerful activator of cytokine genes in immune cells.[21–25] OCT2 expression is highly specific to the B cell lineage, but its expression can be induced by inflammatory signals in both myeloid and lymphoid cell contexts.[7,26,27] This is thought to be explained by *POU2F2* being an NF-κB target gene,[7,27] which allows OCT2 to contribute to the activation of secondary transcriptional responses downstream of inflammatory signals.

One unique mechanism employed by POU TFs OCT1, OCT2, and OCT11/*POU2F3* is their use of specialized transcriptional

coactivators belonging to the OCT coactivator (OCA) protein family.[28,29] Three OCA proteins have been identified to date (OCA-B, OCA-T1, and OCA-T2), each possessing a 23 amino acid segment that binds directly to the DNA-binding domain of POU TFs and with octamer motif (ATGCAAAT) DNA.[29–32] OCA-B expression is highly specific to lymphoid cells,[28,33] where it promotes cell differentiation by functioning as a coactivator of OCT1 and OCT2 at lymphoid-specific genes.[34] By contrast, OCA-T1 and OCA-T2 expression is specific to tuft cells,[29] an important cell type for type II mucosal immunity.[35] In this context, OCA-T1 and OCA-T2 function as OCT11 coactivators to promote tuft cell-specific gene expression.[29]

Here, we show that IκBζ contains a previously overlooked microhomology with the OCA proteins; a 23 amino acid segment that we demonstrate is necessary for binding to POU TFs and octamer motif DNA. We present biochemical, genetic, and epigenomic data supporting that IκBζ is a coactivator of POU TFs, which is mediated by its OCA peptide. Considering the known role of IκBζ in the NF-κB pathway, our findings suggest that the mechanism described here integrates POU TFs with inflammation-induced transcriptional responses.

RESULTS AND DISCUSSION

IκBζ shares a microhomology with OCA-B, OCA-T1, and OCA-T2

We recently identified OCA-T1 and OCA-T2 as tuft cell-specific paralogs of the B cell-specific coactivator OCA-B.[29] All three proteins share a highly conserved N-terminal OCA peptide for binding POU TFs, a less conserved C-terminal trans-activation domain, and are each encoded in a gene cluster on human chromosome 11.[29] Here, we performed a position-specific iterated basic local alignment search tool (PSI-BLAST) analysis in search of additional human proteins that might have an OCA peptide for binding POU TFs, which nominated IκBζ as a candidate (Figures 1A and S1). Unlike the three OCA proteins, IκBζ is encoded on human chromosome 3 and possesses ankyrin repeat domains (Figure 1A). Using a ConSurf analysis,[36] we found that the OCA peptide, like the ankyrin repeat domains, is highly conserved across IκBζ orthologs in different species, suggesting it may have functional importance (Figure 1B). The OCA peptide is present on all annotated IκBζ isoforms, but this sequence is absent on the closest IκBζ paralog B-cell lymphoma-3 (BCL-3) (data not shown). Using the existing X-ray crystal structure of OCA-B bound to OCT1 and DNA[31] (PDB: 1CQT), we generated a homology model substituting IκBζ for OCA-B (Figure 1C). This model predicts shape complementarity and bonding interactions involving IκBζ, OCT1, and DNA, which includes critical bonds that link valines 114/116 with DNA and valine 120 with the POU domain of OCT1 (Figure 1C). Taken together, these analyses led us to hypothesize that IκBζ uses an OCA-like peptide segment to bind to POU TFs.

IκBζ forms a stable complex with POU TFs via its OCA peptide

We next performed biochemical experiments to characterize the putative OCA peptide of IκBζ. Using transient transfection of epitope-tagged proteins in HEK293T cells, we confirmed the ability of OCT2 to co-immunoprecipitate IκBζ in nuclear lysates (Figure 2A). Importantly, a V120E or a V114D/V116D double mutation of IκBζ diminished this interaction, which is consistent with our structural model and with prior mutational studies of the other OCA proteins (Figure 2A).[29] Phenylalanine 111 of the IκBζ OCA peptide is a prominent difference from the three OCA proteins, which instead have a tyrosine at this position (Figure 1A). However, we found that IκBζ^{F111Y} bound to OCT2 in a similar manner to IκBζ^{WT} (Figure 2A). Deletion of the IκBζ ankyrin repeats did not influence the OCT2 interaction (Figure 2A), and, conversely, mutations of the OCA peptide did not influence NF-κB binding (Figure S2A). In this expression system, we found that IκBζ associated with several different POU TFs (e.g., OCT2 and OCT6) but less efficiently with others (e.g., BRN4) (Figure 2B). Using HBL1 cell lysates (see below), we confirmed that endogenously expressed IκBζ associates OCT2 and NF-κB:p50 (Figure S2B). To evaluate whether IκBζ can directly bind to POU TFs, we expressed and purified full-length proteins from bacteria (Figures 2C and S2C). Using pull-down assays and analytical gel filtration, we confirmed that IκBζ (in the presence of octamer motif DNA) selectively and stably binds to OCT1, OCT2, and OCT6 via its OCA peptide (Figures 2D–2G and S2C–S2E). Using these purified proteins, we also found that IκBζ can bridge OCT2 with p50 to form a higher-order complex (Figures S2F and S2G). Taken together, these experiments validate the OCA peptide of IκBζ as a binding surface for POU TFs.

The OCA peptide of IκBζ is required to activate specific immune genes

Prior studies have shown that IκBζ activates inducible immune genes, often by regulating proximal promoter elements.[37–41] In surveying this literature, we noticed that many of the promoters of human IκBζ target genes contained octamer motifs in addition to κB motifs (Figure 3A), albeit with variable levels of evolutionary conservation (Figure S3A). As an example, the IκBζ target *DEFB4A* (encoding an anti-microbial defensin protein) has tandem octamer and κB motifs located ~180 bp upstream of its transcriptional start site (Figure 3A). In accord with prior work,[37] we found that the *DEFB4A* promoter is induced ~50-fold by exposure to tumor necrosis factor alpha (TNF-α) (which activates NF-κB but does not induce IκBζ expression) in combination with transient transfection of IκBζ cDNA constructs in HEK293T cells (Figures 3B, S3B, and S3C). Remarkably, we found that IκBζ-dependent *DEFB4A* activation was eliminated by mutation of conserved valine residues of the OCA peptide or by deletion of the ankyrin repeats, whereas the F111Y mutation behaved like the wild-type protein (Figure 3B). In addition, mutation of the octamer motif, mutation of the κB motif, or a genetic knockout of OCT1 eliminated the inducible activation of *DEFB4A* (Figures 3B–3E and S3D). Similar results were obtained evaluating *ELF3*, which is another IκBζ target gene harboring κB and octamer motifs in its proximal promoter (Figures S3E–S3G).[40] As a control, we found that IκBζ does not require its OCA peptide to activate the promoter of the NF-κB target gene *CXCL8*, which lacks an octamer motif (Figure S3H). Taken together, these findings suggest that IκBζ functions as a coactivator of both NF-κB and POU TFs at inducible immune genes containing recognition motifs for these TFs.

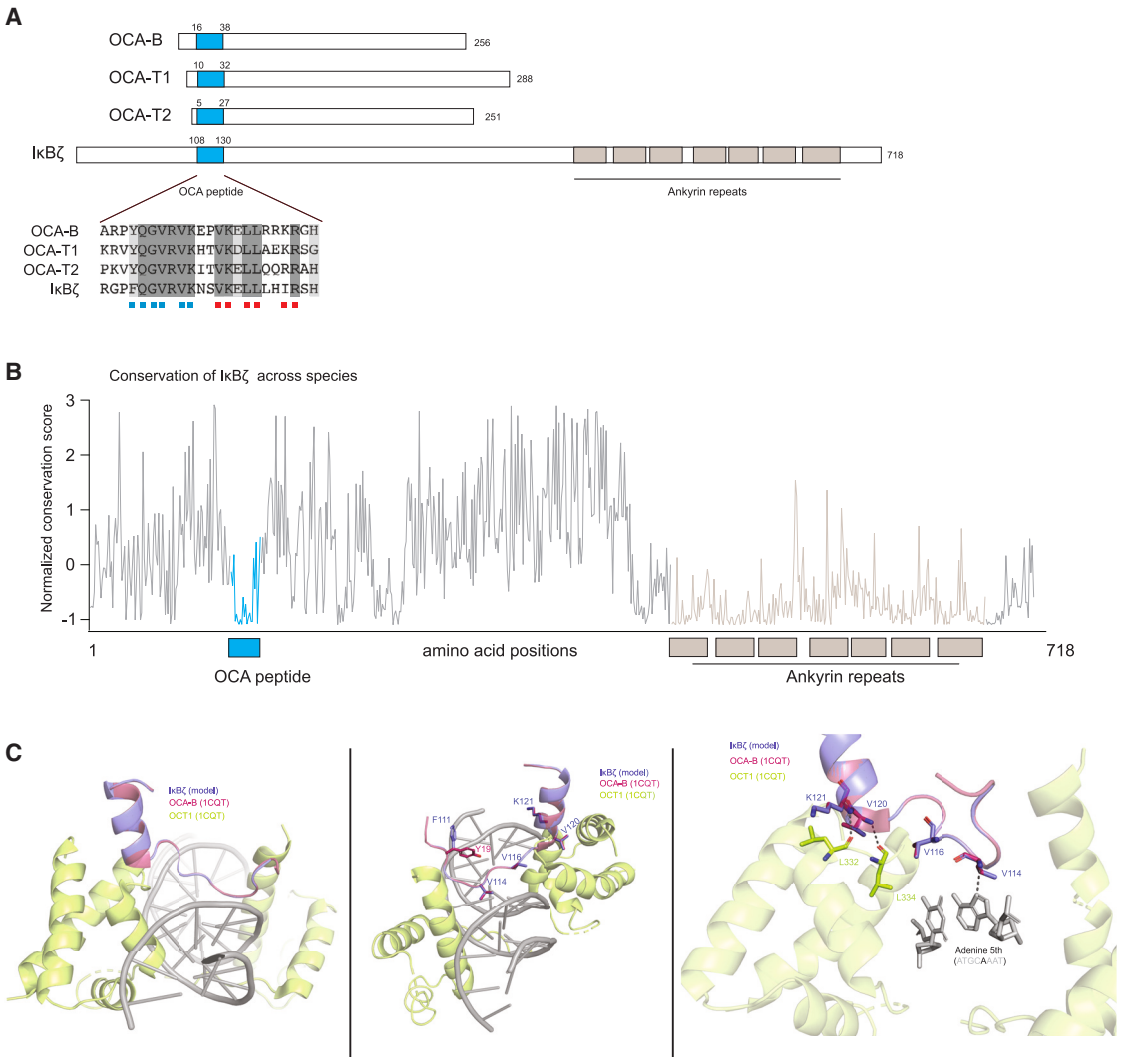

Figure 1. The IκBζ protein has a conserved OCA peptide

(A) Domain architecture of OCA-peptide-containing proteins, OCA-B, OCA-T1, OCA-T2, and IκBζ. OCA peptide (blue box) and ankyrin repeat (beige boxes) are displayed. OCA peptide sequences are retrieved from UniProt and aligned through Clustal Omega. Residues from OCA peptide at DNA interface (blue dots) and POU protein interface (red dots) are marked.

(B) Conservation analysis of IκBζ primary structure across species through the ConSurf Server.

(C) IκBζ segment (residues 109–139) is modeled through Swiss-model using OCA-B-DNA-OCT1 ternary complex (PDB: 1CQT) as template and aligned on the same structure in PyMol. Critical interface residues are labeled on the structure. See also Figure S1.

To explore the generality of this result, we lentivirally expressed IκBζ^{WT} or IκBζ^{V120E} in combination with TNF-α treatment of human lung fibroblasts (Figure 3F), followed by quantitative reverse-transcription PCR (RT-qPCR) analysis of endogenous IκBζ-dependent genes defined in prior studies.[37–41] Although wild-type IκBζ triggered robust activation of this panel of genes, IκBζ^{V120E} was defective at activating *DEFB4A*, *ELF3*, *CSF3*, *IL-10*, *IL-19*, and to a lesser extent *IL-6* (Figures 3G–3L). By contrast, the *LCN2* gene, which lacks an octamer motif in its proximal promoter, was activated independently of the IκBζ OCA peptide (Figure 3M). We obtained similar results in SW982 synovial sarcoma cells treated with TNF-α and transduced with IκBζ cDNAs (Figure S3I). Of note, IκBζ required its OCA peptide to activate *IL-10* and *IL-19*, but this activation did not require TNF-α treatment. The lack of NF-κB-dependence for *IL-10* and *IL-19* expression might be due to the upstream κB motif being greater than 3 kb away from the transcriptional start site. This highlights how different immune genes preferentially rely on NF-κB versus POU TFs for IκBζ-mediated transcriptional activation. Nevertheless, these findings indicate that the inducible activation of specific immune genes relies on the interaction between IκBζ and POU TFs.

Colocalization of IκBζ, OCT2, and NF-kB:p50 in HBL1 lymphoma cells

We next used epigenomics to evaluate the connection between IκBζ and POU TFs. For this purpose, we employed

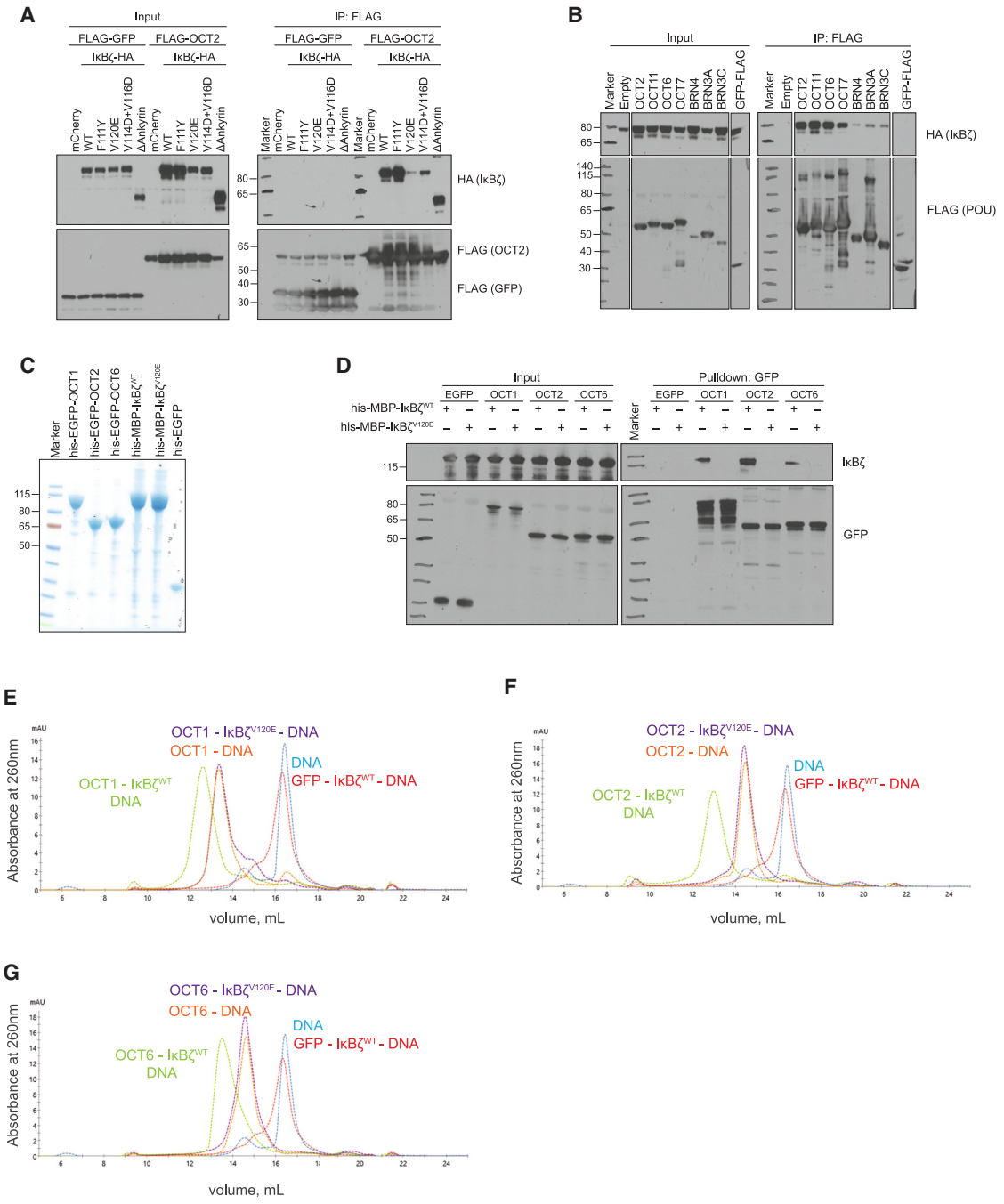

Figure 2. The OCA peptide of IκBζ binds directly to POU TFs

(A) Coimmunoprecipitation-western blotting assay evaluating the effects of substitutions at the OCA peptide or deletion of ankyrin repeats on IκBζ-OCT2 interaction in HEK293T cells.

(B) Coimmunoprecipitation assay testing the ability of different POU transcription factors to interact with IκBζ in HEK293T cells.

(C) Recombinant proteins expressed, affinity-purified, and further purified by size exclusion chromatography and separated on SDS-PAGE gel to evaluate for protein purity.

(D) GFP-pull-down assay with stoichiometric mixtures of tagged POU proteins (OCT1, OCT2, and OCT6), IκBζ (wild-type and V120E mutant), and octamer motif-containing dsDNA.

(E–G) Superposed chromatograms for the gel filtration analysis of various POU-IκBζ assemblies. Absorbance at 260 nm was used as tracer for all separation runs. The same "DNA alone" and "GFP-IκBζ^{WT}-DNA" graphs were used as references in all three comparisons. See also Figure S2.

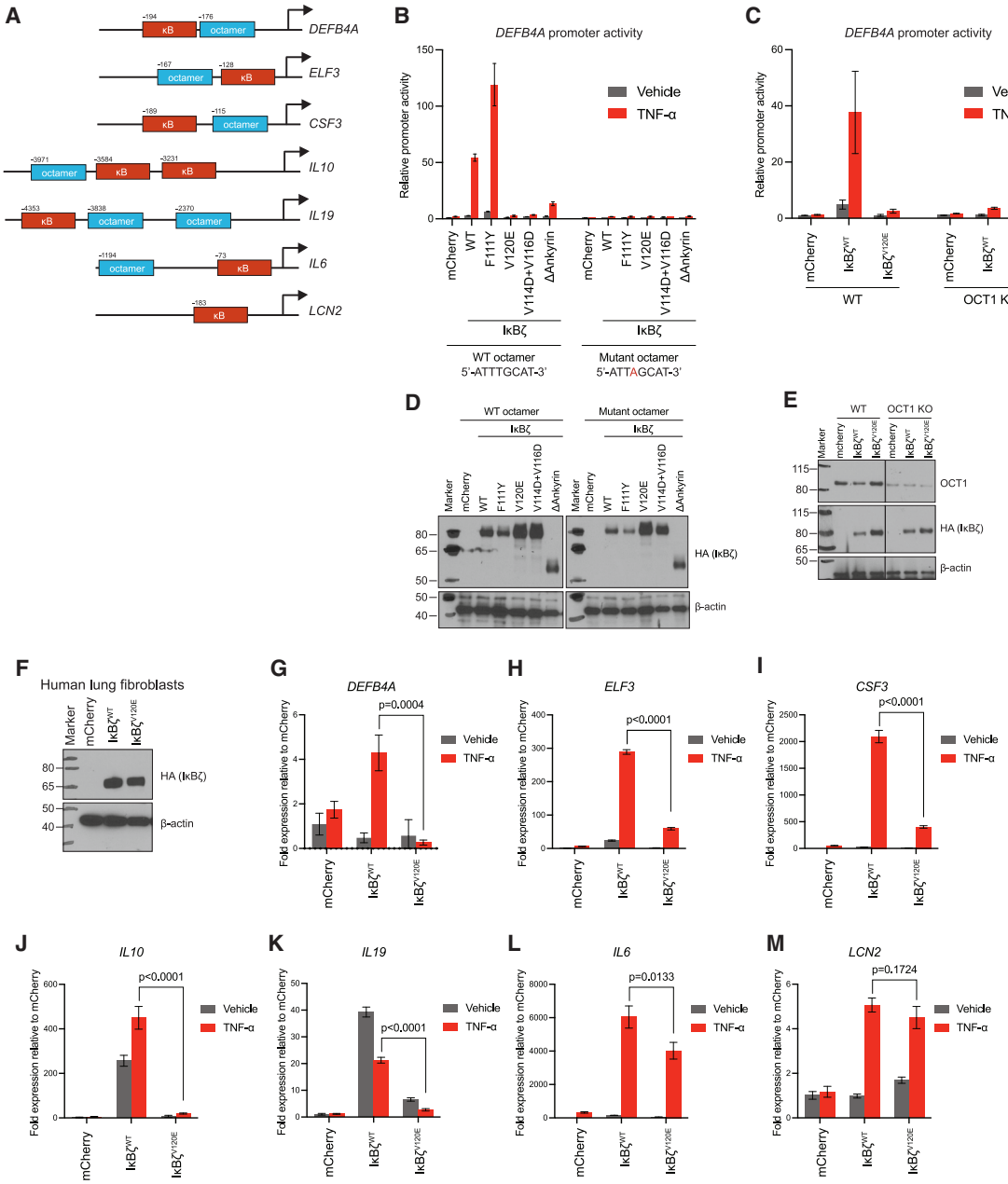

Figure 3. The OCA peptide of IκBζ is required to activate a subset of its immune-related target genes

(A) Diagram of putative promoter regions of select IκBζ target genes. POU octamer motif (blue box) and NF-κB binding site (κB element, red box) are displayed.

(B) *DEFB4A* promoter luciferase activity measured in the presence of reporter plasmids with wild-type octamer motif or mutant octamer motif; IκBζ^{WT} or IκBζ^{V120E}; and in the presence of vehicle or 10 ng/mL TNF-α treated HEK293T cells.

(C) The same activity assay is repeated in control or *POU2F1* (OCT1) knockout HEK293T cells using wild-type octamer reporter. The assays were repeated twice. Data are displayed as mean ± SD of one representative experiment.

(D and E) The post-luciferase assay lysates were separated on SDS-PAGE and blotted with respective antibodies to assess expression levels to ensure that differences in transcriptional activation with the luciferase reporter were not because of diminished protein expression and to ensure the efficiency of CRISPR-based OCT1 knockout.

(F) Western blot analysis of lentiviral HA-tagged IκBζ^{WT} or IκBζ^{V120E} expression in human lung fibroblasts. mCherry cDNA serves as a negative control.

(G–M) RT-qPCR analysis of IκBζ target gene expression in human lung fibroblast cells stably expressing negative control vector, IκBζ^{WT} or IκBζ^{V120E}. The cells were treated with vehicle or 10 ng/mL TNF-α for 24 h before harvesting RNA. RT-qPCR assays were repeated twice. Unpaired Student's t test was used to calculated p values. Data are displayed as the mean ± SD of one representative experiment. See also Figure S3.

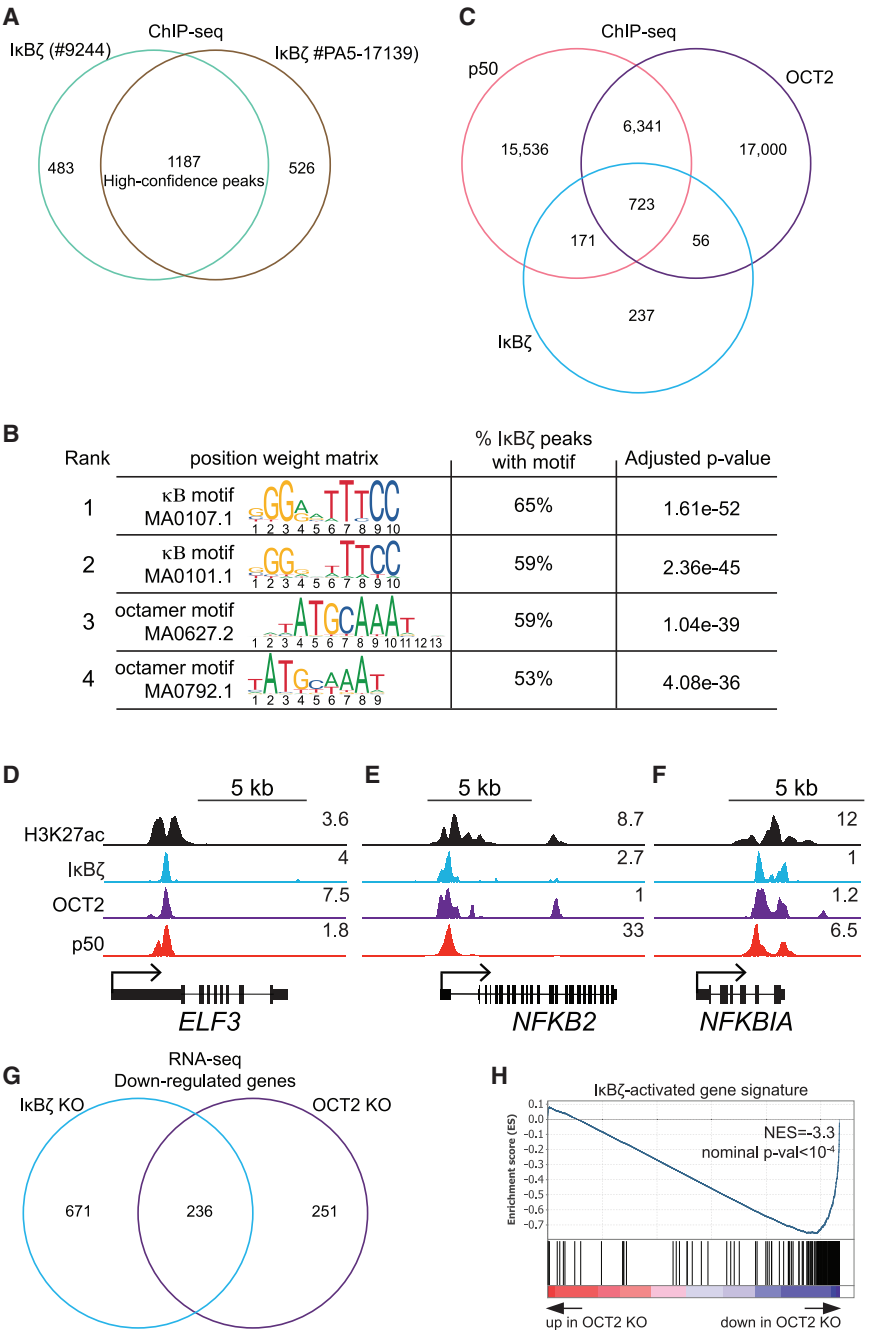

Figure 4. IκBζ colocalizes with OCT2 and NF-κB:p50 at regulatory DNA elements in HBL1 lymphoma cells

(A) Overlap analysis of IκBζ peaks identified by ChIP-seq analysis of HBL1 cells with the two antibodies indicated.

(B) MEME analysis of TF binding motifs enriched within high-confidence IκBζ peaks. The top four motifs are indicated.

(C) Overlap analysis of IκBζ, OCT2, and NF-κB:p50 peaks identified by ChIP-seq analysis of HBL1 cells.

(D–F) Enrichment profiles of H3K27 acetylation, IκBζ, OCT2, and p50 at the indicated genes.

(G) The overlap between significantly down-regulated genes in OCT2 knockout and IκBζ knockout HBL1 cells (padj < 0.1 with 2 TPM threshold).

(H) Gene set enrichment analysis (GSEA) plot of IκBζ knockout signature upon OCT2 knockout. Normalized enrichment score (NES) and nominal p value are indicated. See also Figure S4 and Tables S3, S4, and S5.

the *MYD88*^{L265P}-mutant human diffuse large B-cell lymphoma cell line HBL1. This *MYD88* gain-of-function mutation results in constitutive activation of the NF-κB pathway and leads to high basal expression of IκBζ.[42] As a B cell lineage cancer, HBL1 cells also express OCT2 at high levels.[43] We performed chromatin immunoprecipitation sequencing (ChIP-seq) analysis of IκBζ in HBL1 cells with two independent antibodies to map 1,187 high-confidence binding sites (Figure 4A). Remarkably, a motif enrichment analysis (multiple expectation maximizations for motif elicitation [MEME] suite) revealed κb and octamer motifs as the top-ranked sequence correlates of IκBζ genomic occupancy (Figure 4B). In this analysis, we found that ~65% IκBζ peaks have a κb motif, ~59% of IκBζ peaks have an octamer motif, and ~39% of IκBζ peaks have both motifs (Figure 4B, data not shown). We next performed ChIP-seq analysis of OCT2 and NF-κB:p50 in HBL1 cells. In accordance with the findings above, we found that 61% of IκBζ peaks were enriched for OCT2 and NF-κB:p50, which includes the *ELF3*, *NFKB2*, *NFKBIA*, and *ZNF460* loci (Figures 4C–4F and S4A–S4D). At a smaller subset of DNA elements, we found that IκBζ colocalizes with p50 or OCT2 alone, suggesting that IκBζ can be independently recruited by each TF to specific sites (Figure 4C). This binding pattern is seen at the *EHF* locus, which contains one IκBζ peak colocalized with p50 and another colocalized with OCT2 (Figure S4B). Although the presence of κB and/or octamer motifs explains the majority of IκBζ binding site in the HBL1 genome, our epigenomic and motif analyses suggest that other TFs might also recruit IκBζ to a set of sites independently of NF-κB or POU TFs (Figures 4C and S4E–S4H).

Finally, we evaluated the functional overlap of OCT2 and IκBζ by performing RNA sequencing (RNA-seq) analysis of HBL1 cells followed by CRISPR-based knockout of each factor. From this analysis, we observed that 48% of genes downregulated upon OCT2 knockout (236 out of 487) were also downregulated following knockout of IκBζ (Figure 4G). Moreover, 26% of IκBζ-dependent genes (236 out of 907) were downregulated upon

OCT2 knockout (Figure 4G). This result was further validated using gene set enrichment analysis (GSEA), demonstrating that OCT2 knockout significantly diminishes the expression of genes activated by IκBζ in HBL1 cells (Figure 4H).

Taken together, our findings support a model in which IκBζ functions as a coactivator of NF-κB and POU TFs using its ankyrin repeats and OCA peptide, respectively. Since many inflammation-induced promoters harbor κB and octamer motifs, we speculate that IκBζ recruitment can lead to synergistic transcriptional activation by NF-κB and POU TFs, a least for a subset of target genes. In support of this model, we observe switch-like behavior of the *DEFB4A* promoter, in which NF-κB, OCT1, and IκBζ (using both its OCA peptide and ankyrin repeats) must be present for productive gene activation to occur. This "all-or-nothing" response is reminiscent of the interferon-β (IFN-β) enhanceosome,[44] a DNA element in which exceptional cooperativity exists among TFs bound to this promoter. In this regard, it will be important in future work to determine whether a higher-order complex of IκBζ, NF-κB, and OCT1 is more effective at transcriptional activation than the additive effects of each individual component. Our functional and genomic analyses suggest that the degree of cooperativity among these proteins is likely to be highly gene-specific, with binary NF-κB:IκBζ or POU TF:IκBζ complexes being relevant in specific genomic contexts. Another area of future investigation will be to determine whether additional POU TFs beyond OCT1 and OCT2 also employ IκBζ as a coactivator. Our biochemical findings suggest that OCT6, OCT7, and OCT11 bind to IκBζ, which could regulate immune-related functions in epithelial tissues (e.g., in tuft cells and in the epidermis). Of note, we observe that a significant number of IκBζ binding sites in the genome lack both κb and octamer motifs, suggesting that additional TFs might recruit this cofactor to DNA. In summary, the presence of an OCA peptide on IκBζ suggests a broad integration for POU TFs with NF-κB in mammalian immunobiology.

Limitations of the study

In this study, we describe a novel transcriptional interaction employed by IκBζ using biochemical, genetic, and genomic assays in cell line models of immune-related gene regulation. An important limitation of our study is that we did not address the importance of the IκBζ:POU TF interaction in physiological *in vivo* models of immune cell function, which should be addressed in the future by engineering IκBζ mutations of its OCA peptide in mice. Since POU TFs are highly tissue-specific in their expression pattern, it remains unclear whether the OCA peptide will endow IκBζ with cell-type-specific functionalities, a possibility that warrants further investigation. In addition, since IκBζ is involved in inflammatory diseases (rheumatoid arthritis, psoriasis, eye edema, and colitis) and specific cancer types (diffuse large B cell lymphoma) it will also be important to address the importance of the IκBζ OCA peptide in these contexts.

STAR★METHODS

Detailed methods are provided in the online version of this paper and include the following:

- KEY RESOURCES TABLE
- RESOURCE AVAILABILITY
  - Lead contact
  - Materials availability
  - Data and code availability
- EXPERIMENTAL MODEL AND STUDY PARTICIPANT DETAILS
  - *E.coli* strains
  - Mammalian cell culture
- METHOD DETAILS
  - Position-specific iterated blast analysis
  - Homology modeling of IκBζ
  - Plasmid construction
  - Lentiviral transduction and generation of stable cell lines
  - Western blotting
  - Coimmunoprecipitation
  - Preparation of recombinant proteins
  - GFP pull-down assay
  - Gel filtration assay
  - Analysis of IκBζ target gene promoters for TF motifs
  - Promoter activity assay
  - RT-qPCR
  - ChIP-seq sample preparation
  - ChIP-seq—Data analysis
  - Motif enrichment analysis
  - RNA-seq library preparation
  - RNA-seq analysis
  - Generation of IκBζ-activated gene signature and gene set enrichment analysis
- QUANTIFICATION AND STATISTICAL ANALYSIS

SUPPLEMENTAL INFORMATION

Supplemental information can be found online at https://doi.org/10.1016/j.molcel.2024.01.007.

ACKNOWLEDGMENTS

We thank the Vakoc and Leemor Joshua-Tor lab members for discussions and suggestions throughout the course of this study. We thank the Abdel-Wahab lab for HBL1 cells. This work was supported by the Cold Spring Harbor Laboratory NCI Cancer Center Support grant CA045508. Additional funding was provided to C.R.V. by the Pershing Square Sohn Cancer Research Alliance, National Institutes of Health grants CA013106 and CA242919, Department of Defense grant W81XWH1910317, and the Cold Spring Harbor Laboratory and Northwell Health Affiliation.

AUTHOR CONTRIBUTIONS

A.A. generated the structural model of the OCA peptide (Figure 1), performed biochemical experiments (Figure 2), and performed functional experiments (Figure 3). X.S.W. identified the OCA peptide sequence on IκBζ and generated ChIP-seq libraries shown in Figure 4. S.P. performed biochemical experiments. O.E.D. and O.K. analyzed the ChIP-seq data shown in Figure 4. P.K. purified proteins. B.N. performed cloning of sgRNA constructs. C.R.V. supervised the research and wrote the manuscript.

DECLARATION OF INTERESTS

C.R.V. has received consulting fees from Flare Therapeutics, Roivant Sciences, and C4 Therapeutics; has served on the advisory boards of KSQ

Therapeutics, Syros Pharmaceuticals, and Treeline Biosciences; has received research funding from Boehringer Ingelheim and Treeline Biosciences; and owns stock in Treeline Biosciences.

Received: July 28, 2023
Revised: December 1, 2023
Accepted: January 9, 2024
Published: February 2, 2024

REFERENCES

1. Hayden, M.S., and Ghosh, S. (2012). NF-kappaB, the first quarter-century: remarkable progress and outstanding questions. Genes Dev. *26*, 203–234.
2. Baldwin, A.S., Jr. (1996). The NF-kappa B and I kappa B proteins: new discoveries and insights. Annu. Rev. Immunol. *14*, 649–683.
3. Häcker, H., and Karin, M. (2006). Regulation and function of IKK and IKK-related kinases. Sci. STKE *2006*, re13.
4. Grivennikov, S.I., and Karin, M. (2010). Dangerous liaisons: STAT3 and NF-kappaB collaboration and crosstalk in cancer. Cytokine Growth Factor Rev. *21*, 11–19.
5. Fujioka, S., Niu, J., Schmidt, C., Sclabas, G.M., Peng, B., Uwagawa, T., Li, Z., Evans, D.B., Abbruzzese, J.L., and Chiao, P.J. (2004). NF-kappaB and AP-1 connection: mechanism of NF-kappaB-dependent regulation of AP-1 activity. Mol. Cell. Biol. *24*, 7806–7819.
6. Sepulveda, M.A., Emelyanov, A.V., and Birshtein, B.K. (2004). NF-kappa B and Oct-2 synergize to activate the human 3′ Igh hs4 enhancer in B cells. J. Immunol. *172*, 1054–1064.
7. Tamassia, N., Bianchetto-Aguilera, F., Gasperini, S., Polletti, S., Gardiman, E., Ostuni, R., Natoli, G., and Cassatella, M.A. (2021). Induction of OCT2 contributes to regulate the gene expression program in human neutrophils activated via TLR8. Cell Rep. *35*, 109143.
8. Bendall, H.H., Scherer, D.C., Edson, C.R., Ballard, D.W., and Oltz, E.M. (1997). Transcription factor NF-kappaB regulates inducible Oct-2 gene expression in precursor B lymphocytes. J. Biol. Chem. *272*, 28826–28828.
9. Feng, Y., Chen, Z., Xu, Y., Han, Y., Jia, X., Wang, Z., Zhang, N., and Lv, W. (2023). The central inflammatory regulator IkappaBzeta: induction, regulation and physiological functions. Front. Immunol. *14*, 1188253.
10. Haruta, H., Kato, A., and Todokoro, K. (2001). Isolation of a novel interleukin-1-inducible nuclear protein bearing ankyrin-repeat motifs. J. Biol. Chem. *276*, 12485–12488.
11. Kitamura, H., Kanehira, K., Okita, K., Morimatsu, M., and Saito, M. (2000). MAIL, a novel nuclear I kappa B protein that potentiates LPS-induced IL-6 production. FEBS Lett. *485*, 53–56.
12. Muta, T., Yamazaki, S., Eto, A., Motoyama, M., and Takeshige, K. (2003). IkappaB-zeta, a new anti-inflammatory nuclear protein induced by lipopolysaccharide, is a negative regulator for nuclear factor-kappaB. J. Endotoxin Res. *9*, 187–191.
13. Yamazaki, S., Muta, T., and Takeshige, K. (2001). A novel IkappaB protein, IkappaB-zeta, induced by proinflammatory stimuli, negatively regulates nuclear factor-kappaB in the nuclei. J. Biol. Chem. *276*, 27657–27662.
14. Yamazaki, S., Muta, T., Matsuo, S., and Takeshige, K. (2005). Stimulus-specific induction of a novel nuclear factor-kappaB regulator, IkappaB-zeta, via Toll/Interleukin-1 receptor is mediated by mRNA stabilization. J. Biol. Chem. *280*, 1678–1687.
15. Trinh, D.V., Zhu, N., Farhang, G., Kim, B.J., and Huxford, T. (2008). The nuclear I kappaB protein I kappaB zeta specifically binds NF-kappaB p50 homodimers and forms a ternary complex on kappaB DNA. J. Mol. Biol. *379*, 122–135.
16. Kohda, A., Yamazaki, S., and Sumimoto, H. (2016). The Nuclear Protein IkappaBzeta Forms a Transcriptionally Active Complex with Nuclear Factor-kappaB (NF-kappaB) p50 and the Lcn2 Promoter via the N- and C-terminal Ankyrin Repeat Motifs. J. Biol. Chem. *291*, 20739–20752.
17. Yamamoto, M., Yamazaki, S., Uematsu, S., Sato, S., Hemmi, H., Hoshino, K., Kaisho, T., Kuwata, H., Takeuchi, O., Takeshige, K., et al. (2004). Regulation of Toll/IL-1-receptor-mediated gene expression by the inducible nuclear protein IkappaBzeta. Nature *430*, 218–222.
18. Totzke, G., Essmann, F., Pohlmann, S., Lindenblatt, C., Jänicke, R.U., and Schulze-Osthoff, K. (2006). A novel member of the IkappaB family, human IkappaB-zeta, inhibits transactivation of p65 and its DNA binding. J. Biol. Chem. *281*, 12645–12654.
19. Okuma, A., Hoshino, K., Ohba, T., Fukushi, S., Aiba, S., Akira, S., Ono, M., Kaisho, T., and Muta, T. (2013). Enhanced apoptosis by disruption of the STAT3-IkappaB-zeta signaling pathway in epithelial cells induces Sjogren's syndrome-like autoimmune disease. Immunity *38*, 450–460.
20. Okamoto, K., Iwai, Y., Oh-Hora, M., Yamamoto, M., Morio, T., Aoki, K., Ohya, K., Jetten, A.M., Akira, S., Muta, T., and Takayanagi, H. (2010). IkappaBzeta regulates T(H)17 development by cooperating with ROR nuclear receptors. Nature *464*, 1381–1385.
21. Shakya, A., Kang, J., Chumley, J., Williams, M.A., and Tantin, D. (2011). Oct1 is a switchable, bipotential stabilizer of repressed and inducible transcriptional states. J. Biol. Chem. *286*, 450–459.
22. Hwang, S.S., Kim, L.K., Lee, G.R., and Flavell, R.A. (2016). Role of OCT-1 and partner proteins in T cell differentiation. Biochim. Biophys. Acta *1859*, 825–831.
23. Zhou, L., Nazarian, A.A., Xu, J., Tantin, D., Corcoran, L.M., and Smale, S.T. (2007). An inducible enhancer required for Il12b promoter activity in an insulated chromatin environment. Mol. Cell. Biol. *27*, 2698–2712.
24. Pfeuffer, I., Klein-Hessling, S., Heinfling, A., Chuvpilo, S., Escher, C., Brabletz, T., Hentsch, B., Schwarzenbach, H., Matthias, P., and Serfling, E. (1994). Octamer factors exert a dual effect on the IL-2 and IL-4 promoters. J. Immunol. *153*, 5572–5585.
25. Duncliffe, K.N., Bert, A.G., Vadas, M.A., and Cockerill, P.N. (1997). A T cell-specific enhancer in the interleukin-3 locus is activated cooperatively by Oct and NFAT elements within a DNase I-hypersensitive site. Immunity *6*, 175–185.
26. Kilzheimer, M., Quandt, J., Langhans, J., Weihrich, P., Wirth, T., and Brunner, C. (2015). NF-kappaB-dependent signals control. Eur. J. Immunol. *45*, 3441–3453.
27. Lu, S.C., Chang, S.F., Chen, H.L., Chou, Y.Y., Lan, Y.H., Chuang, C.Y., Yu, W.H., and Chen, C.L. (2007). A novel role for Oct-2 in the lipopolysaccharide-mediated induction of resistin gene expression in RAW264.7 cells. Biochem. J. *402*, 387–395.
28. Luo, Y., Fujii, H., Gerster, T., and Roeder, R.G. (1992). A novel B cell-derived coactivator potentiates the activation of immunoglobulin promoters by octamer-binding transcription factors. Cell *71*, 231–241.
29. Wu, X.S., He, X.Y., Ipsaro, J.J., Huang, Y.H., Preall, J.B., Ng, D., Shue, Y.T., Sage, J., Egeblad, M., Joshua-Tor, L., and Vakoc, C.R. (2022). OCA-T1 and OCA-T2 are coactivators of POU2F3 in the tuft cell lineage. Nature *607*, 169–175.
30. Sauter, P., and Matthias, P. (1998). Coactivator OBF-1 makes selective contacts with both the POU-specific domain and the POU homeodomain and acts as a molecular clamp on DNA. Mol. Cell. Biol. *18*, 7397–7409.
31. Chasman, D., Cepek, K., Sharp, P.A., and Pabo, C.O. (1999). Crystal structure of an OCA-B peptide bound to an Oct-1 POU domain/octamer DNA complex: specific recognition of a protein-DNA interface. Genes Dev. *13*, 2650–2657.
32. Babb, R., Cleary, M.A., and Herr, W. (1997). OCA-B is a functional analog of VP16 but targets a sparate surface of the Oct-1 POU domain. Mol. Cell. Biol. *17*, 7295–7305.
33. Shakya, A., Goren, A., Shalek, A., German, C.N., Snook, J., Kuchroo, V.K., Yosef, N., Chan, R.C., Regev, A., Williams, M.A., and Tantin, D. (2015). Oct1 and OCA-B are selectively required for CD4 memory T cell function. J. Exp. Med. *212*, 2115–2131.
34. Teitell, M.A. (2003). OCA-B regulation of B-cell development and function. Trends Immunol. *24*, 546–553.

35. Schneider, C., O'Leary, C.E., and Locksley, R.M. (2019). Regulation of immune responses by tuft cells. Nat. Rev. Immunol. *19*, 584–593.

36. Yariv, B., Yariv, E., Kessel, A., Masrati, G., Chorin, A.B., Martz, E., Mayrose, I., Pupko, T., and Ben-Tal, N. (2023). Using evolutionary data to make sense of macromolecules with a "face-lifted" ConSurf. Protein Sci. *32*, e4582.

37. Johansen, C., Bertelsen, T., Ljungberg, C., Mose, M., and Iversen, L. (2016). Characterization of TNF-alpha- and IL-17A-Mediated Synergistic Induction of DEFB4 Gene Expression in Human Keratinocytes through IkappaBzeta. J. Invest. Dermatol. *136*, 1608–1616.

38. Hörber, S., Hildebrand, D.G., Lieb, W.S., Lorscheid, S., Hailfinger, S., Schulze-Osthoff, K., and Essmann, F. (2016). The Atypical Inhibitor of NF-kappaB, IkappaBzeta, Controls Macrophage Interleukin-10 Expression. J. Biol. Chem. *291*, 12851–12861.

39. Johansen, C., Mose, M., Ommen, P., Bertelsen, T., Vinter, H., Hailfinger, S., Lorscheid, S., Schulze-Osthoff, K., and Iversen, L. (2015). IkappaBzeta is a key driver in the development of psoriasis. Proc. Natl. Acad. Sci. USA *112*, E5825–E5833.

40. Kouri, V.P., Olkkonen, J., Nurmi, K., Peled, N., Ainola, M., Mandelin, J., Nordström, D.C., and Eklund, K.K. (2023). IL-17A and TNF synergistically drive expression of proinflammatory mediators in synovial fibroblasts via IkappaBzeta-dependent induction of ELF3. Rheumatol. Oxf. Engl. *62*, 872–885.

41. Slowikowski, K., Nguyen, H.N., Noss, E.H., Simmons, D.P., Mizoguchi, F., Watts, G.F.M., Gurish, M.F., Brenner, M.B., and Raychaudhuri, S. (2020). CUX1 and IkappaBzeta (NFKBIZ) mediate the synergistic inflammatory response to TNF and IL-17A in stromal fibroblasts. Proc. Natl. Acad. Sci. USA *117*, 5532–5541.

42. Nogai, H., Wenzel, S.S., Hailfinger, S., Grau, M., Kaergel, E., Seitz, V., Wollert-Wulf, B., Pfeifer, M., Wolf, A., Frick, M., et al. (2013). IkappaBzeta controls the constitutive NF-kappaB target gene network and survival of ABC DLBCL. Blood *122*, 2242–2250.

43. Hodson, D.J., Shaffer, A.L., Xiao, W., Wright, G.W., Schmitz, R., Phelan, J.D., Yang, Y., Webster, D.E., Rui, L., Kohlhammer, H., et al. (2016). Regulation of normal B-cell differentiation and malignant B-cell survival by OCT2. Proc. Natl. Acad. Sci. USA *113*, E2039–E2046.

44. Maniatis, T., Falvo, J.V., Kim, T.H., Kim, T.K., Lin, C.H., Parekh, B.S., and Wathelet, M.G. (1998). Structure and function of the interferon-beta enhanceosome. Cold Spring Harb. Symp. Quant. Biol. *63*, 609–620.

45. Tarumoto, Y., Lu, B., Somerville, T.D.D., Huang, Y.H., Milazzo, J.P., Wu, X.S., Klingbeil, O., El Demerdash, O., Shi, J., and Vakoc, C.R. (2018). LKB1, Salt-Inducible Kinases, and MEF2C Are Linked Dependencies in Acute Myeloid Leukemia. Mol. Cell *69*, 1017–1027.e6.

46. Kuroda, A., Rauch, T.A., Todorov, I., Ku, H.T., Al-Abdullah, I.H., Kandeel, F., Mullen, Y., Pfeifer, G.P., and Ferreri, K. (2009). Insulin gene expression is regulated by DNA methylation. PLoS One *4*, e6953.

47. Lu, B., Klingbeil, O., Tarumoto, Y., Somerville, T.D.D., Huang, Y.H., Wei, Y., Wai, D.C., Low, J.K.K., Milazzo, J.P., Wu, X.S., et al. (2018). A Transcription Factor Addiction in Leukemia Imposed by the MLL Promoter Sequence. Cancer Cell *34*, 970–981.e8. e978.

48. Tarumoto, Y., Lin, S., Wang, J., Milazzo, J.P., Xu, Y., Lu, B., Yang, Z., Wei, Y., Polyanskaya, S., Wunderlich, M., et al. (2020). Salt-inducible kinase inhibition suppresses acute myeloid leukemia progression in vivo. Blood *135*, 56–70.

49. Waterhouse, A., Bertoni, M., Bienert, S., Studer, G., Tauriello, G., Gumienny, R., Heer, F.T., de Beer, T.A.P., Rempfer, C., Bordoli, L., et al. (2018). SWISS-MODEL: homology modelling of protein structures and complexes. Nucleic Acids Res. *46*, W296–W303.

STAR★METHODS

KEY RESOURCES TABLE

REAGENT or RESOURCE	SOURCE	IDENTIFIER
Antibodies		
Mouse Anti-HA-HRP Clone 6E2	Cell Signaling Technology	Cat# 2999; RRID:AB_1264166
Mouse monoclonal anti-FLAG-HRP clone M2	Sigma-Aldrich	Cat# F3165; RRID:AB_259529
Goat polyclonal anti-GFP	Abcam	Cat# ab6673; RRID:AB_305643
Rabbit polyclonal anti-OCT1 (POU2F1)	Thermo Scientific	Cat# PA5-28209; RRID:AB_2545685
Rabbit polyclonal anti-IkB zeta (IκBζ) (ChIP-seq, WB)	Thermo Scientific	Cat# PA5-17139; RRID:AB_10985253
Rabbit IκB-ζ Antibody (ChIP-seq)	Cell Signaling Technology	Cat# 9244; RRID:AB_2151602
Mouse monoclonal anti-β-Actin, HRP-linked	Sigma-Aldrich	Cat# A3854; RRID:AB_262011
Rabbit polyclonal anti-H3K27Ac (ChIP-seq)	Abcam	Cat# ab4729; RRID:AB_2118291
Rabbit polyclonal anti-OCT2 (ChIP-seq)	Proteintech	Cat# 10867-2-AP; RRID:AB_2167080
Rabbit monoclonal anti-p105/p50 (ChIP-seq)	Cell Signaling Technology	Cat# 13586; RRID:AB_2665516
Rabbit polyclonal anti-RelA (p65)	Fortis Life Sciences	Cat# A301-824A; RRID:AB_1264341
Rabbit monoclonal anti-p50/p105	Thermo Scientific	Cat# MA5-41097; RRID:AB_2898851
Mouse monoclonal NFκB p50 Antibody (E-10) HRP-linked	Santa Cruz	sc-8414 HRP; RRID:AB_628015
Bacterial and virus strains		
BL21-CodonPlus (DE3)-RIPL Competent Cells	Agilent	Cat# 230280
One Shot™ BL21(DE3)	Invitrogen	Cat# C600003
Chemicals, peptides, and recombinant proteins		
TNF-α	R&D Systems	Cat# 210-TA-005
IL-17A	R&D Systems	Cat# 7955-IL-025
Polyethylenimine, Linear, MW 25,000 (PEI 25000) [for DNA transfection]	Polysciences	Cat# 23966–1
TransIT®-LT1 Transfection Reagent	Mirus Bio	MIR 2304
Hexadimethrine bromide (polybrene)	Sigma-Aldrich	Cat# H9268
Puromycin dihydrochloride	Sigma-Aldrich	Cat# P8833
Zeocin	Thermo Scientific	Cat# R25001
Anti-FLAG® M2 Magnetic Beads	Sigma Aldrich	Cat# M8823
TRIzol Reagent	Thermo Scientific	Cat# 15596018
SuperScript™ IV VILO™ Master Mix	Thermo Scientific	Cat# 11756050
PowerUp™ SYBR™ Green Master Mix for qPCR	Thermo Scientific	Cat# A25918
β-Mercaptoethanol	Sigma-Aldrich	Cat# M6250
ChromoTek GFP-Trap® Magnetic Particles M-270	Proteintech	Cat# gtd
Pierce™ Lane Marker Reducing Sample Buffer	Thermo Scientific	Cat# 39000
RIPA buffer	Thermo Scientific	Cat# 89900
AcquaStain Protein Gel Stain	Bulldog Bio	Cat# AS001000
PrimeStar GXL polymerase	Takara	Cat# R050A
Lysozyme	Thermo Scientific	Cat# 89833
Ni-NTA Agarose	Qiagen	Cat# 30230
Poly(ethyleneimine) solution [for protein purification]	Sigma-Aldrich	Cat# P3143
Blasticidin S HCl	Thermo Scientific	Cat# A1113903
Opti-MEM®	Thermo Scientific	Cat# 31985062
Protein A Dynabeads	Thermo Scientific	10002D
Protein G Dynabeads	Thermo Scientific	10004D
Ribonuclease A (RNase A) from bovine pancreas	Sigma-Aldrich	R4875

(*Continued on next page*)

Continued

REAGENT or RESOURCE	SOURCE	IDENTIFIER
Formaldehyde, 37% solution	Avantor	2106-01
Proteinase K	New England Biolabs	P8107S
AMPure XP beads	Beckman Coulter	A63881
Critical commercial assays		
Firefly & Renilla Luciferase Single Tube Assay Kit	Biotium	Cat# 30081-1
In-Fusion® Snap Assembly Master Mix	Takara	Cat# 638947
QIAquick PCR purification kit	Qiagen	Cat# 28104
NEBNext Ultra II DNA Library Prep Kit for Illumina	New England Biolabs	Cat# E7645
Qubit dsDNA HS Assay Kit	Thermo Scientific	Q32854
NEBNext Poly(A) mRNA Magnetic isolation module	NEB	E7350
NEBNext Ultra II RNA Library Prep kit for Illumina	NEB	E7770
Deposited data		
RNA-seq and ChIP-seq	This paper	NCBI GEO: GSE239374
Uncropped western blot images	This paper	Mendeley dataset: https://doi.org/10.17632/4xm52ybv3g.1
Experimental models: Cell lines		
Human: SW982	ATCC	HTB-93
Human: hTERT lung fibroblasts	ATCC	CRL-4058
Human: HEK293T	ATCC	CRL-3216
Human: HBL1	Gift from Omar Abdel Wahab	N/A
Oligonucleotides		
sgRNA sequences, see Table S1	This paper	N/A
Primers for RT-qPCR, see Table S2	This paper	N/A
22-mer octamer sequence for GFP pull-down and gel filtration assays: GATGTCTGAATGCAAATTTTAC	Wu et al.[29]	N/A
Recombinant DNA		
MGC Human NFKBIZ Sequence-Verified cDNA	Horizon	MHS6278-202806212
MGC Human POU2F2 Sequence-Verified cDNA	Horizon	MHS6278-202829867
LRG2.1	Tarumoto et al.[45]	Addgene plasmid # 108098, RRID:Addgene_108098
LRG2.1T Zeocin	This study	N/A
pGL410_INS421	Kuroda et al.[46]	Addgene plasmid # 49057
pHAGE Empty	Lu et al.[47]	N/A
pMD2.G, vsvg encoding plasmid	Didier Trono (unpublished)	Addgene Plasmid #12259, RRID:Addgene_12259
psPAX2	Didier Trono (unpublished)	Addgene plasmid # 12260, RRID:Addgene_12260
lentiV_Cas9_Puro	Tarumoto et al.[45]	Addgene plasmid # 108100, RRID:Addgene_108100
lentiV_Cas9_Blast	Tarumoto et al.[48]	Addgene plasmid # 125592, RRID:Addgene_125592
pET28b-6×His-ECFP	This study; Wu et al.[29]	N/A
pET28b-8×His-MBP	This study	N/A
pRSFDuet-1	Novagen	Cat# 71341-3
Software and algorithms		
GraphPad Prism 9.5.1 (528)	GraphPad Prism, Inc	https://www.graphpad.com/
PyMOL 2.5.4	Schrödinger	https://pymol.org/2/
R software (4.1.1)	R Project	https://www.r-project.org/

RESOURCE AVAILABILITY

Lead contact

Further information and requests for resources and reagents should be directed to and will be fulfilled by the lead contact, Christopher Vakoc (vakoc@cshl.edu).

Materials availability

All unique reagents generated in this study will be available from the lead contact upon request.

Data and code availability

RNA-seq and ChIP-seq data have been deposited at NCBI GEO with accession GSE239374. Accession numbers are listed in the key resources table. Original western blot images have been deposited at Mendeley and will be publicly available as of the date of publication. The DOI is listed in the key resources table.

This paper does not report original code.

Any additional information required to reanalyze the data reported in this paper is available from the lead contact upon request.

EXPERIMENTAL MODEL AND STUDY PARTICIPANT DETAILS

E.coli strains

BL21 (DE3) cells were used in this study to produce recombinant proteins.

Mammalian cell culture

Human hTERT-transformed lung fibroblast cell line, SW982 synovial sarcoma cell line and HEK293T cells were obtained from ATCC. These lines are cultured in DMEM supplemented with 10% FBS, extra L-Glutamine and penicillin/streptomycin. HBL1 cells (a gift from the Abdel-Wahab lab) were cultured in RPMI supplemented with 10% FBS. All cell lines were maintained at 37 °C with 5% CO_2 and were periodically tested for mycoplasma contamination.

METHOD DETAILS

Position-specific iterated blast analysis

The OCA peptide of OCA-B/POU2AF1 was analyzed for homology with the human proteome using the BlastP suite with the PSI-Blast algorithm using standard settings. https://blast.ncbi.nlm.nih.gov/Blast.cgi?PROGRAM=blastp&PAGE_TYPE=BlastSearch&BLAST_SPEC=&LINK_LOC=blasttab&LAST_PAGE=blastp. Output is shown in Figure S1.

Homology modeling of IκBζ

IκBζ (Uniprot: Q9BYH8-1; residues 109-139) structure was predicted using the existing OCA-B structure (PDB: 1CQT) as template in SWISS-MODEL.[49] The IκBζ model was superposed to OCA-B with OCT1 (PDB: 1CQT) in PyMol (2.5.4) and the IκBζ residues at the DNA and OCT1 interfaces were inferred.

Plasmid construction

MGC Human NFKBIZ (IκBζ) Sequence-Verified cDNA (MHS6278-202806212) and MGC Human POU2F2 (OCT2) Sequence-Verified cDNA (MHS6278-202829867) were obtained from Horizon. The coding sequence of OCT6 (Genebank: NM_002699.4) and codon-optimized versions of BRN3A (Uniprot: Q01851), BRN3C (Uniprot: Q15319) and BRN4 (Uniprot: P49335) for *E.coli* expression were synthesized by Twist Biosciences. Mammalian expression vectors for OCT11, BRN3C and BRN4 constructs were obtained from Wu et al.[29] For expression in mammalian cells, the ORF sequences were cloned into pcDNA3.1 or pHAGE-puro vector with a C-terminal 3×HA tag (for IκBζ) or N-terminal 3×FLAG tag (POU proteins). For IκBζ, the point mutations and ankyrin repeat deletion were introduced by site-directed mutagenesis. For recombinant protein expression in bacteria, full-length $IκBζ^{WT}$ or $IκBζ^{V120E}$ were cloned into pET28 vector with 8×His-MBP tag. Full-length OCT2, OCT6, and codon-optimized BRN ORFs (BRN3A, BRN3C and BRN4) were cloned into pET28 vector with N-terminal 6×His-ECFP tag. 6×His-EGFP tagged OCT1 was obtained from Wu et al.[29] Truncated p50 (amino acids 41–352) was cloned with an N-terminal 7×His tag into pRSF Duet-1 vector.

For reporter assays with POU2F1/OCT1 knockout, LRG2.1T Zeo was derived from LRG2.1T Neo (Addgene Plasmid #125593) by replacing neomycin cassette with bleomycin (zeocin) resistance cassette from pTRE:CloverCP-EFS:ZeoR (Addgene Plasmid #68478). Single guide RNAs (sgRNAs) were cloned by annealing two single-stranded oligonucleotides and ligating annealed oligos into BsmBI-digested LRG2.1 Zeo vector. For knockout cell lines in HBL1, single guide RNAs were cloned into LRG2.1 (Addgene Plasmid #108098) using the same cloning strategy as LRG2.1 Zeo. The sgRNA sequences used in the study are listed in Table S1.

Lentiviral transduction and generation of stable cell lines

Lentivirus for SpCas9 expression [lentiV-Cas9-Blast (Addgene Plasmid #125592) or lentiV-Cas9-Puro (Addgene Plasmid #108100)], single sgRNA expression or expression of IκBζ constructs were prepared by transfecting HEK293T cells. Briefly, 7 million HEK293T cells were plated into 10 cm dish one day before the transfection. Next day, 6 μg transfer plasmid, 4.5 μg psPAX2 (Addgene Plasmid # 12260) and 1.5 μg pMD2.G (encodes vsvg, Addgene Plasmid #12259) were mixed in 600 μL Opti-MEM. Thirty six μL of 1 mg/mL Polyethylenimine (PEI 25000) was added and vortexed. Transfection mixture was incubated 20 minutes at room temperature before transferred over the HEK293T cells. 8-12 hour post-transfection, the growth medium was exchanged with fresh complete medium. Virus containing medium was collected 48 hours after medium replacement; spined at 300×g at room temperature for 5 minutes and filtered through 0.45 μm SFCA filters (Corning). Filtered viral supernatant was mixed with appropriate growth medium and 4 μg/mL polybrene; transferred over the target cells and spinfected for 40 minutes at 32°C, 600×g. Medium was refreshed 48 hours-post-infection and selected with appropriate antibiotics until non-infected cells were dead.

In order to knockout OCT1, HEK293T cells were first infected with Cas9 virus and selected with 10 μg/mL blasticidin to generate stable HEK293TCas9. Next, HEK293TCas9 was infected with LRG2.1T Zeo viruses with negative control sgRNA or sgRNA that targeted OCT1 and selected with 500 μg/mL zeocin. Human lung fibroblast cells and SW982 were infected with pHAGE-puro lentivirus encoding mCherry, $IκBζ^{WT}$ or $IκBζ^{V120E}$. Medium was refreshed 48 hours-post-infection. SW982 cells were selected with 1 μg/mL puromycin until non-infected cells were dead. HBL1 cells stably expressing Cas9 were generated by lentiviral transduction of lentiV-Cas9-Puro. For selecting HBL1 Cas9 cells, single clone was picked and the Cas9 editing efficiency was validated by growth arrest phenotype upon *CDK1* knockout. Three Cas9 efficient editing clones were combined for IκBζ or OCT2 knockout experiments.

Western blotting

Whole cell lysates were prepared in RIPA buffer and protein concentrations were determined using BCA assay (Pierce) according to manufacturer's directions. Equal amounts of proteins were mixed with protein sample buffer and separated in 4-12% Bis-Tris precast gels (Thermo Scientific). The separated proteins were then transferred onto nitrocellulose membrane, blocked with 5% nonfat milk in 1×TBS+0.15%Tween 20 (TBST) for an hour at room temperature. The membrane was then probed with primary antibodies o/n and then –if necessary– with HRP-conjugated secondary antibodies. Rinsed membranes were then treated with ECL substrate and exposed to X-ray films. Antibodies used in western blotting are mouse anti-HA-HRP Clone 6E2 (Cell Signaling Technology, Cat# 2999), mouse monoclonal anti-FLAG-HRP clone M2 (Sigma-Aldrich, Cat# F3165), goat polyclonal anti-GFP (Abcam, Cat# ab6673), rabbit polyclonal anti-OCT1 (POU2F1) (Thermo Scientific, Cat# PA5-28209), rabbit polyclonal anti-IkB zeta (IκBζ) (Thermo Scientific, Cat# PA5-17139), mouse monoclonal anti-β-Actin, HRP-linked (Sigma-Aldrich, Cat# 07-473), rabbit polyclonal anti-RelA (p65) (Fortis Life Sciences, Cat# A301-824A) and rabbit monoclonal anti-p50/p105 (Thermo Scientific, Cat#MA5-41097).

Coimmunoprecipitation

HEK293T cells transiently expressing 3×FLAG-tagged POU proteins or 3×HA tagged IκBζ were grown in 10cm dishes. Approximately ~10 million were harvested by trypsinization. The cells were pelleted by centrifugation at 300×g for 5 minutes at room temperature. The cell pellet was washed twice in cold PBS and transferred into 1.5 mL centrifuge tubes. The cells were gently lysed in 900 μL buffer A (10 mM HEPES pH 7.9, 5 mM magnesium acetate, 1 mM $MgCl_2$, 0.3 M sucrose, 0.1% NP-40, protease inhibitors and 0.2 mM PMSF) and incubated on ice for 15 minutes. Nuclei were pelleted by spinning at 9800×g for 10 minutes at 4 °C. The supernatant was removed, and the nuclear pellet was resuspended in 1 mL co-IP buffer (25 mM HEPES pH 7.9, 10% Glycerol, 0.8% NP-40, 2 mM magnesium acetate, 350 mM NaCl and protease inhibitors). The extracts were incubated with gentle rotation at 4 °C for 30 minutes and the insoluble chromatin was pelleted by centrifuging at 21000×g for 40 minutes at 4 °C. The supernatant containing the nuclear extract was carefully transferred into a fresh centrifuge tube and 2% (v/v) was taken as input. Twenty-five microliters of magnetic Flag-M2 beads (Sigma) was transferred into fresh centrifuge tubes and washed twice in 400 μL co-IP buffer. Equal volumes of cleared extracts were transferred on washed beads and rotated 16 hours at 4 °C. The beads were washed three times with 1 mL co-IP buffer; resuspended in 1x SDS sample buffer and boiled for 5 minutes for elution. Eluted proteins and input fractions were separated and detected as discussed in Western blot section. For co-IP with endogenous IκBζ protein in HBL1 cells, whole cell lysate was prepared in lysis buffer (20 mM Tris–Cl pH 8, 20% glycerol, 2 mM EDTA, 150 mM KCl), supplemented with 0.1% NP-40, protease inhibitor cocktail, 0.7 μl/ml β-mercaptoethanol and PMSF. The whole cell lysates were then precleared with 25 μl of Protein A magnetic beads by incubating at 4°C for 1-2 hours. In a separate tube, 25 μl of Protein-A magnetic beads were blocked with 1.5% BSA by incubating at 4°C for 1-2 hours. The blocked beads were further washed three times with wash buffer (20 mM Tris–Cl pH 8, 20% glycerol, 2 mM EDTA, 150 mM KCl), supplemented with 0.1% NP-40. The washed pre-blocked beads were then incubated with 2 μg anti-IκBζ and control IgG antibodies for 6-8 hours at 4°C. The precleared cell lysates were subsequently incubated with the antibody conjugated beads for 14-16 hours at 4°C. The beads were then washed three times and the immunoprecipitated samples were heat eluted in 2x Laemmli buffer by incubating at 98°C for 8-10 minutes. The interactions among the proteins were investigated by western blotting.

Preparation of recombinant proteins

Sequence-validated plasmids except pRSF-Duet-7×His-p50(41-352) were transformed into BL21-CodonPlus (DE3)-RIPL competent cells. OCT1, OCT2, OCT6, BRN3A, BRN3C, BRN4 and IκBζ cultures were grown in LB media until $OD_{λ=600}$ reaches 0.8-1.

The cultures were cooled down at 4°C and induced with 0.2 mM IPTG at 16°C for 16 hours. pRSF-Duet-7×His-p50(41-352) plasmid was transformed into One Shot™ BL21(DE3). The bacterial culture was grown in LB media until OD $_{\lambda=600}$ reaches 0.4-0.5. After cooling down at 4°C, the culture was induced with 0.15 mM IPTG at 18°C for 16-18 hours. Bacterial cultures were harvested by centrifuging at 4600×g for 15 minutes at 4 °C and pellets were stored at -20 °C until lysis.

Frozen pellets of OCT1, OCT2, OCT6, BRN3A, BRN3C and BRN4 cultures were thawed and resuspended in lysis buffer I (50 mM Tris-phosphate pH 7.9, 500 mM NaCl, 10% glycerol, 20 mM imidazole, 10 mM 2-merchaptoethanol, 0.2 mM PMSF, and protease inhibitor cocktail). IκBζ^{WT} or IκBζ^{V120E} were extracted in lysis buffer II (50 mM Tris-phosphate pH 7.7, 500 mM NaCl, 2 mM MgOAc2, 3 mM MgCl2, 10% glycerol, 1% Tween 20, 50 mM imidazole, 10 mM 2-merchaptoethanol, 0.2 mM PMSF, and protease inhibitor cocktail). The lysates are supplemented with 0.5 mg/mL lysozyme; incubated on ice for 10 minutes and then sonicated. 0.1% PEI was added to sonicated crude lysate to further deplete nucleic acids. The crude lysate was clarified by centrifugation using F21-8 x 50y fixed-angle rotor (Thermo Scientific) at 38 000×g, 4 °C for 1 hour. The clarified lysates were then applied onto Ni-NTA beads (Qiagen) and washed with respective lysis buffers and then wash buffer (50 mM Tris-phosphate pH 7.5, 150 mM NaCl and 20 mM imidazole). The bound proteins were then eluted using 50 mM Tris-phosphate pH 7.5, 150 mM NaCl, 250 mM imidazole. Eluates were supplemented with 1 mM EDTA and 1 mM DTT and concentrated with Amicon centrifugal filters. The purified proteins were further polished with size exclusion chromatography using Superdex 200 increase (Cytiva) in 50 mM sodium phosphate pH 7.5, 150 mM NaCl, 1 mM EDTA. For p50 purification, frozen pellets were thawed and lysed in lysis buffer III (20 mM Tris pH 7.5, 150 mM NaCl, 20 mM Imidazole 1 mM DTT, 0.2 mM PMSF, and protease inhibitor cocktail). The lysates are supplemented with 0.5 mg/mL lysozyme; incubated on ice for 10 minutes and then sonicated. The crude lysate was clarified by centrifugation using T-865 fixed-angle rotor (Thermo Scientific) at 40 000×rpm, 4 °C for 1 hour. The clarified lysates were then applied onto Ni-NTA beads (Qiagen) and extensively washed with lysis buffer III. The protein was eluted using lysis buffer III with 250 mM imidazole. Eluates were supplemented with 1 mM EDTA and 1 mM DTT and concentrated with Amicon centrifugal filters. The concentrated protein was further purified by running through Superdex 200 increase column using 50 mM HEPES pH 7.6, 150 mM NaCl, 1 mM EDTA as run buffer. The elution volume matched with the size of a homodimer based on the separation of standard proteins. Size and purity of the preparations were assessed by SDS-PAGE separation followed by Coomassie blue staining.

GFP pull-down assay

Five hundred nanomolar of IκBζ^{WT} or IκBζ^{V120E} was mixed with 200 nM 22-mer octamer motif containing dsDNA and 200 nM EGFP, OCT1, OCT2, OCT6, BRN3A, BRN3C or BRN4 in binding buffer (50 mM Tris pH 7.5, 150 mM NaCl, 0.2% Brij35 and 1 mM DTT). GFP-Trap® Magnetic Particles M-270 (Chromotek) was added on the binding mixtures and nutated for 5 hours at 4°C to pull down OCT proteins or EGFP. The beads were quickly rinsed three times in the binding buffer. The proteins bound to beads were eluted with 2x Laemmli buffer. The association of IκBζ and POU proteins were assessed by western blotting. To test IκBζ-mediated interaction between OCT2 and NFκB p50, pull-down assay conditions were slightly modified. Briefly, approximately 2 μg of bait proteins (EGFP or tagged-OCT2) were incubated with 3 μg his-p50 (41-352) in absence or presence of 2 μg tagged IκBζ^{WT} or IκBζ^{V120E}. The proteins were incubated in binding buffer containing 20 mM Tris–Cl pH 8, 20% glycerol, 2mM EDTA, 100 mM KCl; supplemented with 0.08% NP-40 and BSA (20ng/ul). 25μl ChromoTek GFP-Trap® Magnetic Agarose bead along with 22-mer octamer motif containing dsDNA were added to the reaction mixtures and incubated for 12 hours at 4°C. The beads were subsequently washed three times with binding buffer and the bead bound proteins were eluted in 2× Laemmli buffer by boiling. The interactions among the proteins were investigated by western blotting.

Gel filtration assay

One and a half micromolar of tagged IκBζ^{WT} or IκBζ^{V120E} was mixed with 1 μM 22-mer octamer motif containing dsDNA and 1.2 μM EGFP, OCT1, OCT2 or OCT6 in size exclusion buffer (10 mM HEPES pH 7.5, 25 mM ammonium acetate, 1 mM DTT) and incubated for 5 minutes at room temperature. Two hundred and fifty microliters of the binding mixture was injected into Superdex 6 increase column (Cytiva) and separated in the size exclusion buffer with 0.6 mL/min flow rate. Chromatograms (with absorbance at 260 nm as tracer) of individual runs of the same POU TF were superposed and relative elution volumes of various sets of complexes were compared.

Analysis of IκBζ target gene promoters for TF motifs

The upstream sequences of select IκBζ target genes were retrieved from Ensemble (release 109, Feb 2023) and Eukaryotic Promoter Database (EPD, Expasy). For NFKB1, the motif matrix was obtained from JASPAR (NFKB1, ID: MA0105.1). For class II POU motifs, the consensus octamer sequence (′-ATGCAAAT-3′) was used. The locations of putative TF motifs were assigned using FIMO tool (MEME Suite 5.5.3) and filtered based on whether these sites were functionally validated previously.

Promoter activity assay

The genomic sequences upstream of *DEFB4A* TSS (382 bp), *ELF3* TSS (338 bp) and *CXCL8* TSS (499 bp) were cloned upstream of firefly luciferase gene in pGL410 vector. The octamer motif (ATGCAAAT) was mutated by substituting thymidine in place of 5th adenine by site-directed mutagenesis to generate mutant octamer motif-containing reporters. κB motif perturbations were depicted underneath relevant graphs. A total of 82 ng of plasmids encoding various derivatives of IκBζ or mCherry; 15 ng of pGL410 reporter

plasmid and 3 ng of Renilla luciferase encoding plasmid were diluted in 9 μL Opti-MEM medium and mixed with 0.3 μL TransIT-LT1 transfection reagent (Mirus Bio). The transfection mixture added dropwise on top of HEK293T cells (25000 cells/ well in a 96-well plate) and incubated for 19 hours. The cells were treated with 10 ng/mL TNF-a or PBS for 5 hours. Firefly & Renilla Luciferase Single Tube Assay Kit (Biotium) was used according to manufacturer's directions to assess the relative luciferase activity.

RT-qPCR

Human lung fibroblasts and SW982 stably expressing mCherry, IκBζ^{WT} or IκBζ^{V120E} were plated in a 6-well plate. The next day, the growth medium was replaced with serum-free medium and further incubated for 16 hours. The cells were treated with 10 ng/mL TNF-α or PBS for additional 24 hours (fibroblasts) or 8 hours (SW982) and harvested into TRIzol (Thermo Scientific). Total RNA was prepared as recommended and 500 ng total RNA was used for reverse-transcription with SuperScript™ IV VILO™ Master Mix (Thermo Scientific). Quantitative PCR was prepared with diluted RT reactions, target-specific primer pairs and PowerUP qPCR master mix (Thermo Scientific) and performed in QuantStudio™ 6 Flex Real-Time PCR System (Thermo Scientific). RT-qPCR data was normalized to *ATP5F1*, *GAPDH* and *ACTB* genes and expressed as fold change over empty vector according to $2^{-\Delta\Delta Ct}$ method. Statistical analysis was performed using ΔΔCt values through unpaired t-test between "IκBζ^{WT} + TNF-α" and "IκBζ^{V120E} + TNF-α" samples. RT-qPCR primers are listed in Table S2.

ChIP-seq sample preparation

For each ChIP, 20 million cells were used. Cells were cross-linked with 1% formaldehyde for 10 min at room temperature with agitation and quenched with 0.125 M glycine for 5 min at room temperature. After washing twice with PBS, cells were incubated in 1 ml cell lysis buffer (10 mM Tris-HCl (pH 8.0), 10 mM NaCl, 0.2% NP-40 with protease inhibitor) for 15 min on ice. Nuclei were isolated by centrifugation at 600×g for 30 s, resuspended in 1 ml nuclear lysis buffer (50 mM Tris-HCl (pH 8.0), 10 mM EDTA, 1% SDS with protease inhibitor) and sonicated using a Bioruptor Pico (Diagenode) (30s on/off, 10 cycles). In all cases, the chromatin was centrifuged at maximum speed in a tabletop centrifuge for 15 min at 4 °C. The supernatant was mixed with 7 ml IP dilution buffer (20 mM Tris-HCl (pH 8.0), 2 mM EDTA, 150 mM NaCl, 1% Triton X-100), and incubated with the indicated antibody for 2 h. Protein A/G magnetic beads (25 μl, Dynabeads, Thermo Fisher Scientific) were washed twice with PBS and added to the antibody–chromatin mixture at 4 °C overnight. The beads were washed once with IP wash 1 buffer (20 mM Tris-HCl pH 8.0, 2 mM EDTA, 50 mM NaCl, 1% Triton X-100, 0.1% SDS), twice with high salt buffer (20 mM Tris-HCl (pH 8.0), 2 mM EDTA, 500 mM NaCl, 1% Triton X-100, 0.01% SDS), once with IP wash 2 buffer (10 mM Tris-HCl pH 8.0, 1 mM EDTA, 250 mM LiCl, 1% NP-40, 1% sodium deoxycholate) and twice with TE (pH 8.0). Chromatin DNA was eluted, and cross-linking was reversed in 200 μl nuclear extraction buffer with 12 μl of 5 M NaCl and 1 μg /mL RNase A at 65 °C overnight. The beads were then discarded. The DNA-containing supernatant was treated with 4 μg /mL proteinase K at 56 °C for 20 min and purified using the QIAquick PCR purification kit (QIAGEN) in 60 μl water.

For ChIP-seq of H3K27Ac (Abcam, ab4729, 2 μg in total), 5 million cells were used; for IκBζ ChIP–seq (CST #9244S and Invitrogen Cat #PA5-17139, 2 μg per IP), 5 ChIP samples were pooled before IP wash one and 2 ug antibody were used for each ChIP; for OCT2 (Proteintech 10867 and Abcam ab178679) and p50 (CST #13586S), 2 IP reactions were combined before IP wash one and 2.5 μg antibody was used for each ChIP. ChIP-seq libraries were prepared using the NEBNext Ultra II DNA Library Prep Kit for Illumina (E7645) according to the manufacturer's protocol with AMPure XP beads (Beckman Coulter, A63881) with no size selection. One extra amplification cycle was added to final PCR enrichment. The final PCR product was cleaned using AMPure XP beads twice. Library quality was assessed via Bioanalyzer equipped with the high-sensitivity DNA chip (Agilent) and quantified using the Qubit dsDNA HS Assay Kit (Thermo Fisher Scientific, Q32854). ChIP-seq libraries were pooled and analysed by single-end sequencing 76-bp sequencing using the NextSeq (Illumina) system.

ChIP-seq—Data analysis

Sequencing reads were mapped to the human genome (hg38) using Bowtie2 (2.4.4). Duplicate read removal and sorting was performed using SAMtools (1.14). Peaks were called using MACS2 (2.2.7.1) broad peak (H3K27ac) or narrow peak (p50, OCT2, IκBζ) option using FDR cut off 5%. Big wig files were generated using deepTools (3.5.1). ChIP-seq tracks were generated using UCSC genome browser. The nearest expressed gene (>2 transcripts per million, TPM) assignment was performed using HOMER. The list of peak positions, the nearest gene positions and IDs are provided in Table S3.

Motif enrichment analysis

DNA sequences for high-confidence IκBζ were extracted using BEDtools (2.29) and background files and shuffled sequence control files were generated (MEME Suite 5.5.3). For motif enrichment analysis the AME tool (MEME Suite 5.5.3) was used. A motif library with 883 vertebrate TF position weight matrices (JASPAR2022 core vertebrates) was scanned across the 1,187 peak regions and motifs were ranked by p value. FIMO tool (p value = 0.001) was used together with the top 4 motif (two kb and two octamer motifs) to identify peaks with kb, octamer or both motifs.

RNA-seq library preparation

For knockout experiments, cells were collected 6 days after infection with sgRNA for HBL1 Cas9 cells. Total RNA was extracted using TRIzol (Thermo Fisher Scientific) according to the manufacturer's protocol and resuspended in RNase-free water. Poly(A) RNA

was selected and fragmented with NEBNext Poly(A) mRNA Magnetic isolation module (NEB, E7350) and the library was prepared using the NEBNext Ultra II RNA Library Prep kit for Illumina (NEB, E7770) with 2 μg RNA according to the manufacturer's protocol. RNA-seq libraries were pooled and analysed by single-end 76 bp sequencing using the NextSeq (Illumina) system.

RNA-seq analysis

Raw reads were aligned to the human transcriptome (GRCh38-release 108) using Kallisto (v 0.46.1). For differential gene expression analysis, read counts were analyzed using DESeq2 (v. 1.40.2), comparing knockout samples of IκBζ and OCT2 to control sgROSA with 5 different guides as biological replicates for the IκBζ knockout, 3 different guides for OCT2 knockout, and 2 different guides for sgROSA. A technical replicate was also used for each sample, and the two technical replicates were combined in the transcript quantification step in Kallisto. The differential expression gene analysis was performed using a gene expression cutoff of >2 TPM. Significantly down- or up-regulated genes were determined using a cut of p.adj <0.1 in DESeq2, and are provided in Table S4.

Generation of IκBζ-activated gene signature and gene set enrichment analysis

Genes were ranked based on differential gene expression following IκBζ knockout and the top 200 downregulated genes were selected as "IκBζ-activated gene signature" (gene list provided in Table S5). The differentially expressed gene list following OCT2 knockout was analyzed using gene set enrichment analysis (weighted GSEA Pre-ranked tool v4.3.2). 1,000 gene set permutations were applied and the IκBζ-activated gene signature was used as gene set.

QUANTIFICATION AND STATISTICAL ANALYSIS

GraphPad PRISM version 9.5.1. was used to generate the graphs and perform the statistical analysis in Figures 3 and S3. Data were plotted as mean ± standard deviation (SD). All experimental assays were performed in duplicate or triplicate. RT-qPCR data (Figures 3 and S3) were analyzed through unpaired two-tailed t test, as detailed in figure legends and respective STAR Methods section. P values were depicted on the figures and $p<0.05$ was considered statistically significant. Bioinformatics-associated analyses (Figures 4 and S4) were performed in R (version 4.1.1) using the tools, algorithms, and software indicated in respective STAR Methods section. Cutoff values and other statistical parameters were indicated in figure legends, figures, and respective STAR Methods section.